Optical properties of silicon and its oxides

C. Tarrio* and S. E. Schnatterly

Jesse W. Beams Laboratory of Physics, University of Virginia, Charlottesville, Virginia 22901

Received July 13, 1992; revised manuscript received November 30, 1992

We have measured the inelastic electron scattering spectra of a variety of Si and SiO_2 thin films from the fundamental absorption threshold to well above the L-shell thresholds. We have used Kramers–Kronig analyses and sum rules to obtain the dielectric and optical response functions. We compare the optical properties of crystalline and evaporated and hydrogenated amorphous Si, amorphous evaporated SiO and SiO_2, and chemical-vapor-deposition SiO_2 in both the interband and the L-shell absorption regions. The interband structure in crystalline Si shows three sharp peaks that are blended into a single broad peak in the amorphous samples. At the L threshold crystalline Si also shows more structure than amorphous Si, however, the overall shape in the region well above the threshold is quite similar in the three samples. Above the SiO_2 band gap the three oxide samples show strikingly similar behavior.

INTRODUCTION

Si and its oxides have been extensively studied. Besides their importance in the semiconductor industry, Si and the Si–SiO_2 systems are becoming increasingly important as electron[1] and photon[2] detectors. The central role of the optical properties of the materials contained in electron and photon detectors makes it necessary to have an accurate knowledge of these properties over a wide energy range.[1,2]

In past studies of the optical properties of Si most of the attention has focused on the IR to near UV range.[3–6] The extensive measurements on crystalline Si (c-Si) have resulted in a good understanding of the optical properties, although surface preparation has been found to be crucial in determining accurate values of the dielectric functions.[6] The results for amorphous Si (a-Si) have indicated a strong dependence on the method of preparation. Vacuum evaporation can be used to prepare a-Si, which results in a sample of low mass density and high defect density. The quality of the sample can be improved by the introduction of H, which passivates some of the dangling bonds. Hydrogenated Si (a-Si:H) can be prepared either by glow discharge or by chemical vapor deposition. If one varies the deposition conditions, the H content of these samples can be varied from ~6 to over 50 at. %.[4]

Some reflectance studies have included Kramers–Kronig (KK) analyses to obtain values of the complex dielectric function.[3,4] However, because of the narrow energy range covered in many of the experiments (usually 1–6 eV), uncertainties that are due to extrapolation at high energy are introduced. The need for broad-range data for determining the dielectric function is eliminated by ellipsometry measurements, which have been made for both c-Si[6,7] and a-Si.[7,8]

Inelastic electron scattering (IES) spectra obtained at small transverse momentum can also yield dielectric functions through a KK analysis. Results have been reported for c-Si in the range of the interband transitions and plasma losses.[9] There have also been IES measurements of the momentum dependence of the plasmon peak.[10,11] In the region of the L edge, optical absorption measurements have been performed on c-Si and a-Si,[12,13] and IES measurements have also been reported.[14]

Although much experimental and theoretical attention has been paid to the optical properties of SiO_2 and SiO, these materials are less well understood than Si. The central reason for this lack of understanding is the complicated crystal stuctures, the difficulty in preparing pure, single-phase samples, and the small dielectric constant of SiO_2, which leads to a large electron–hole interaction, and hence optical properties that differ significantly from single-particle calculations. Reflectance measurements into the vacuum UV have been reported for both stoichiometric and nonstoichiometric Si oxides.[15] Dielectric functions of α-quartz have been obtained from IES measurements,[16] while $L_{2,3}$ spectra have been obtained from optical absorption[13] and IES.[17] Core spectra probing the valence and the conduction states independently have also been reported.[18]

Because of the complications mentioned above, considerable confusion exists over the band gap of SiO_2, which varies by a few electron volts in the literature. Some techniques can be used that simplify the interpretation of experimental results. Examples of such experiments include field-dependent photoconductivity, which measured a gap of 9.3 eV for fused quartz,[19] and temperature-dependent Urbach absorption, which found 8.7 eV for vitreous silica and 9.1 eV for α-quartz.[20] Temperature-dependent measurements found 2.6 eV for SiO.[21]

We have measured IES spectra of c-Si, a-Si, and a-Si:H, as well as a-SiO, a-SiO_2, and chemical-vapor-deposition (CVD) of SiO_2 from the IR to over 400 eV. Through a KK analysis we have obtained reliable values of the dielectric and optical constants. This is the first study to cover such a broad energy range on a single instrument, which thus eliminates the uncertainties of patching together data from different instruments, and the first to cover the difficult region between 40 and 100 eV. We compare the behavior of the c-Si and a-Si samples in both the interband

0740-3224/93/050952-06$05.00

and L_{23} absorption regions. We also compare SiO and SiO_2 in these two regions, and we discuss defect absorption in the two SiO_2 samples.

BACKGROUND

In the high-energy limit the Born approximation holds for IES spectroscopy, leading to the cross section[22]

$$\frac{d^2\sigma}{d\omega d\Omega} \propto \frac{1}{q^2}\,\mathrm{Im}\left[\frac{-1}{\epsilon(q,\omega)}\right], \tag{1}$$

where q is the wave vector of the excitation, ω is the frequency, and $\epsilon = \epsilon_1 + i\epsilon_2$ is the complex longitudinal dielectric function. In the limit $q \to 0$, the longitudinal and transverse (optical) dielectric functions become equal. At low energy the most commonly measured optical property in semiconductors is the reflectivity:

$$R(\omega) = \left|\frac{N(\omega)-1}{N(\omega)+1}\right|^2 = |r(\omega)\exp[i\theta(\omega)]|^2, \tag{2}$$

where $N = n + ik = \sqrt{\epsilon}$ is the complex index of refraction, r is the amplitude of the reflected wave relative to the incident wave, and θ is the phase. At high energies, R becomes negligible. In this case the absorption coefficient, $\alpha(\omega) = 2\omega k(\omega)/c$, which falls off only as ω^{-2}, is the more commonly measured quantity.

IES, reflectivity, and optical absorption probe different attributes of the sample, yet they can all be related to one another through the KK relations.[23] Since all the KK integrals are evaluated over all frequencies, it is important to cover as broad an energy range as possible to obtain reliable dielectric functions. In any experiment one must assume some functional form of the data in order to extrapolate to infinite energy; however, the broader the energy range of the measurement, the better the results will be.

There are two major differences between electron and optical spectroscopy. The first is the ability of electrons to excite bulk plasmons, collective longitudinal oscillations of the electron gas. The second is the ability to vary the energy loss and momentum transfer independently. In the case of IES this allows us to study peak dispersion and nonvertical transitions, which are not accessible by means of optical techniques, which are constrained to near-zero wave-vector excitations.

EXPERIMENTAL

Measurements were made on the IES accelerator described in Ref. 24. Energy loss was controlled by a precision power supply and calibrated regularly through measurements of the zero-energy-loss maximum. Energy losses of less than 1 eV to over 400 eV were covered with a resolution of ~0.1 eV. The primary beam energy was 280 keV. Transverse momentum transfer was delivered by high-voltage capacitor plates and was calibrated by measurements of well-known diffraction peaks. Momentum transfers of 0.07 to 1.2 $Å^{-1}$ were covered with a resolution of ~0.04 $Å^{-1}$.

Measured spectra contain kinematic effects resulting from the energy dependence of the longitudinal momentum transfer. The spectra also contain multiple scattering events in which a single fast electron scatters more than once in the sample. We used algorithms of Livins *et al.*[25] to remove these effects. At low energy, owing to the large index of refraction, Čerenkov radiation is prominent in the spectra of Si. In c-Si we corrected for Čerenkov effects by scaling the ellipsometry data of Aspnes and Studna[6] to our spectra at ~5 eV. In a-Si, because of the higher count rate and the strong dependence of the optical properties on sample preparation, we have not used published data to remove Čerenkov contributions.

The c-Si sample was a single crystal thinned chemically and argon-ion milled to an appropriate thickness. The a-Si:H sample was grown by rf decomposition of 16.7% SiH_4 in Ar, with a substrate temperature of 254 °C.[26] The sample was deposited onto a NaCl substrate and floated off in deionized water before being picked up onto an electron microscope grid. The a-Si samples were grown by electron-beam vacuum evaporation onto NaCl and also floated off in H_2O. The pressure in the vacuum chamber was between 10^{-7} and 10^{-6} Torr. All the samples were ~550 Å thick. SiO and SiO_2 samples were also vacuum evaporated onto NaCl. Another SiO_2 sample was prepared by CVD of SiH_4 in an O_2 atmosphere. The sample was deposited onto GaAs and floated off in a H_2SO_4–H_2O_2 solution. The evaporated oxide samples were ~300 Å thick, and the CVD sample was ~800 Å thick.

DISCUSSION

Plasmons

A plasmon is a collective oscillation of an electron gas. For an electron gas a simple analysis leads to the equation $\omega_p^2 = 4\pi ne^2/m$, where ω_p is the plasma frequency and n is the electron density. For a simple metal such as Na or Al, this expression is quite accurate. In semiconductors, however, the effect of interband transitions, which shift the plasmon to higher energy, must be included[27]:

$$\omega_p^2 = \frac{4\pi ne^2}{m} + \omega_0^2, \tag{3}$$

where ω_0 is an excitation energy. The plasmon energy is expected to disperse quadratically with momentum[28]:

$$\omega_p(q) = \omega_p(0) + \frac{\hbar^2}{m}\alpha q^2. \tag{4}$$

In the random-phase approximation the dispersion coefficient is $\alpha = 3E_F/(5\hbar\omega_p)$, where E_F is the Fermi energy. The introduction of electron correlations reduces the predicted dispersion[29]:

$$\alpha = \frac{3E_F}{5\hbar\omega_p}\left[1 - \frac{1}{16}\left(\frac{\hbar\omega_p}{E_F}\right)^2\right]. \tag{5}$$

Figure 1 shows the absolute energy loss functions of the three Si samples obtained at low momentum. These spectra should agree with results obtained by optical techniques. Each sample shows a clear plasmon peak near 16.7 eV, characterized by an upward zero crossing in ϵ_1. As expected in semiconductors in which the loss peak is well above interband losses, the loss function has a Drude free-electron shape at low momentum. The zero crossings in ϵ_1 are also at energies slightly lower than the loss peaks.

To obtain plasmon dispersion data, we have fitted Drude shapes to the loss spectra. This step was necessary for us to obtain plasmon widths, because of the increase in single-particle excitations at higher momenta. The dis-

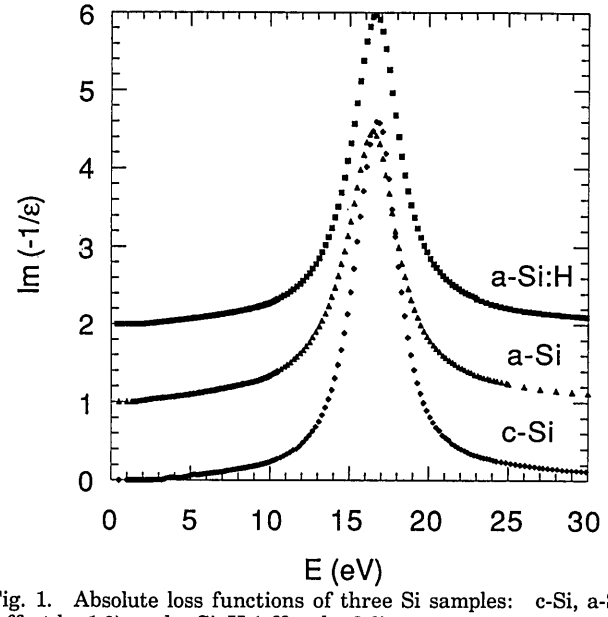

Fig. 1. Absolute loss functions of three Si samples: c-Si, a-Si (offset by 1.0), and a-Si:H (offset by 2.0).

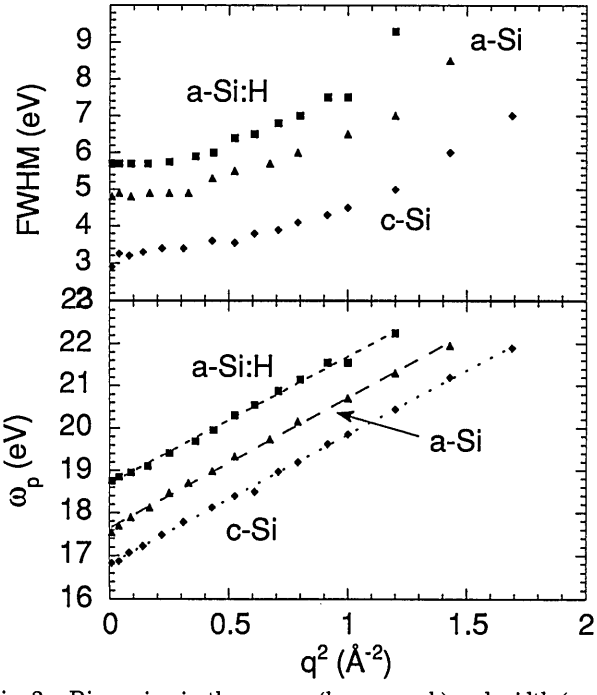

Fig. 2. Dispersion in the energy (lower graph) and width (upper graph) of the plasmons in c-Si, a-Si (offset by 1 eV), and a-Si:H (offset by 2 eV).

persion in the energies and widths of the plasmons for the three samples are shown in Fig. 2. The plasmon peak dispersion is clearly quadratic. Parabolas were fitted to the dispersion data to yield values of $\omega_p(0)$ and α. These values, along with the predictions of the above models, are shown in Table 1. To obtain theoretical values of α, we have evaluated Eq. (5) with a Fermi energy of 12.4 eV (Ref. 30) and our measured values of $\omega_p(0)$. The values predicted by Eq. (5) are in surprising agreement with our data. As expected, $4\pi ne^2/m$ somewhat underestimates the plasma frequency. Equation (3) is difficult to evaluate because of the imprecise definition of ω_0. If we assume that ω_0 is the peak energy in the ϵ_2 spectra, then our values of ω_p from Eq. (3) are in no better agreement with our measurements.

The plasmon width dispersion data are quite interesting. None of the three samples shows the quadratic behavior present in many materials. This is to be expected in the amorphous samples. Disordered and dirty samples often show a decrease in the plasmon width with increasing momentum at low to moderate wave vectors. In such cases the intercept of the high-q linear region is close to the zero-q width in the pure material. In our amorphous data we do not observe a decrease in width, but a constancy at low to moderate momentum. Moreover, extrapolation of the high-q data does not yield the zero-q width of the c-Si plasmon. The rather large width (3 eV) of the plasmon at low q in c-Si is due to interband transitions, which are still quite strong at 16 eV. The q dependence of the width is then due primarily to the effects of interband transitions and is evidently more complex than the above phenomenological model.

Interband Transitions

The upper portion of Fig. 3 shows our ϵ_2 spectra of c-Si with the ellipsometry results of Aspnes and Studna,[6] which were used for low-energy extrapolation. The spectra both show three peaks; however, ours has the amplitudes of the first two peaks reversed. This may seem

Table 1. Calculated and Experimental Values for the Plasma Frequencies and Dispersion Coefficients of Three Silicon Samples

Sample	$4\pi ne^2/m$ (eV)	ω_p Meas. (eV)	α Calc.	α Meas.
c-Si	16.60	16.79	0.39	0.40
a-Si	15.76	16.63	0.40	0.38
a-Si:H	16.13	16.69	0.40	0.37

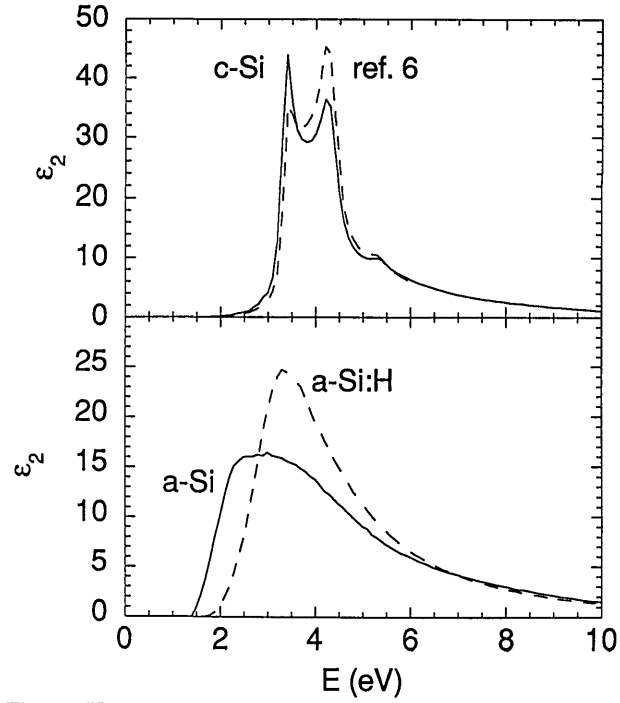

Fig. 3. Upper graph: ϵ_2 of c-Si. The solid curve is the authors' measurement, and the dashed curve is ellipsometry data from Ref. 6. Lower graph: ϵ_2 of a-Si and a-Si:H.

surprising; however, to patch their data to our own, we calculated $\mathrm{Im}(-1/\epsilon) = \epsilon_2/(\epsilon_1^2 + \epsilon_2^2)$ and scaled this factor to our raw spectra. In the region of the interband transitions the dielectric function is large and rapidly varying, leading to a smaller cross section and reduced sensitivity to sharp features in energy-loss measurements relative to ellipsometry and other optical techniques. Čerenkov radiation, still present in the electron spectra at the upper limit of the ellipsometry data, also may play a role in the accuracy of scaling and patching of our data to the ellipsometry data. Small errors in patching the loss function are exaggerated in the ϵ_2 spectra through the KK analysis.

The lower curves in Fig. 3 are our ϵ_2 spectra for the amorphous samples. We have not extrapolated these data with published data because of the strong dependence of the optical properties on sample preparation and the greater signals in the amorphous materials. We have assumed typical dielectric constants of 12.0 for a-Si and 11.5 for a-Si:H.[31] Our a-Si sample shows a band gap of 1.45 eV, and a-Si:H, 1.75 eV. The peak energy in a-Si of 3.0 eV and the amplitude of 16 in ϵ_2 are somewhat lower than previous measurements.[5] This discrepancy is most likely due to our preparation conditions, leading to a sample of low density and dielectric constant. The peak in the a-Si:H spectrum is at 3.3 eV, with an amplitude of approximately 25. This is similar to reflectivity results obtained on a film prepared under similar conditions.[5] In addition to the uncertainty in our a-Si spectra that is due to the lack of dielectric constant measurements, there is the uncertainty that is due to Čerenkov radiation, which is undoubtedly present, and the large value of ϵ_1, which makes the electron cross section small. Therefore comparison of our results to previous studies is fairly positive.

L-Shell Losses

In the energy region near the L-shell absorption, our values of ϵ_1 differ from unity by less than 0.03, making $\mathrm{Im}(-1/\epsilon)$, ϵ_2, and $2k$ all approximately equal. In the soft-x-ray range the most commonly measured quantity is the optical transmission, $I = I_0 \exp(-\alpha t)$, where I and I_0 are the transmitted and incident x-ray intensities and t is the sample thickness. In such measurements uniform sample thicknesses are required to obtain accurate values for the absorption coefficient. However, IES spectroscopy relies on detecting only electrons that have lost energies, so nonuniformities and even pinholes in samples do not greatly affect our measurements.

When one considers absorption from core levels in the single-particle approximation, the joint density of states J_{cv} reduces to a transition density of states from the narrow width of the initial state. Thus the absorption from the $2p$ level probes the s- and d-like unoccupied density of states. Based on the behavior of the interband transitions, we expect the L_{23} absorption to be similar in the crystalline and the amorphous samples, with the exception of some additional fine structure in the crystalline sample. Figure 4 shows the absorption coefficients for the three samples in the L_{23} absorption region. In c-Si the absorption coefficient has been shown to differ significantly from theoretical predictions based on accurate band structure calculations.[32] This difference is most likely due to the presence of excitonic effects, which shift oscillator strength to lower energies.[33] The major difference between the crystalline and amorphous spectra other than the fine structure from 100–110 eV is in the apparent $p_{3/2}$ to $p_{1/2}$ ratio at the absorption edge, found by fitting two error functions to the spin–orbit partners near threshold. The expected ratio of about 2:1 is evident in the amorphous samples, but additional structure near the threshold in c-Si makes it appear as though that ratio were approximately 1:1.

RESULTS: OXIDES

The constituent atoms of SiO and SiO_2 are the same, yet their band gaps and dielectric constants are quite different, and thus one may expect both similarities and differences in their spectra. Figure 5 shows the loss functions for evaporated SiO and SiO_2 and for CVD SiO_2. As can be seen, the spectra are remarkably similar above the SiO_2 band gap. None of the oxides shows an upward zero crossing in ϵ_1 near the dominant peak in the loss function; the minimum in ϵ_1 of ~0.5 occurs at ~18 eV in each sample. This leads to a plasma enhancement peak at 22.5 eV in SiO and 23.5 eV in SiO_2. The absence of a true plasmon peak is due to the strength of interband transitions at high enough energies to cause overdamping of the plasma resonance. The lower density of O $2s$ electrons in SiO is probably the cause of the somewhat greater amplitude in the plasma enhancement peak and the smaller loss function in the region above 30 eV.

Figure 6 shows ϵ_2 in the interband region for the three materials. Above the SiO_2 band gap the spectra are similar, as are the loss functions. The SiO_2 spectra show peaks at 10.25, 11.7, 13.6, and 16.8 eV. The SiO spectrum shows a peak at 10.2 eV and features at approximately

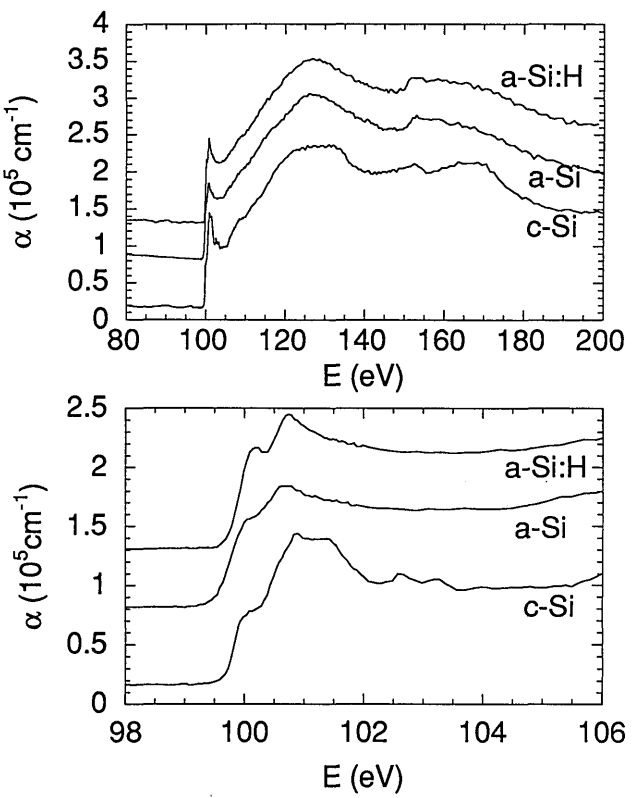

Fig. 4. Absorption coefficient of c-Si, a-Si (offset by 0.5×10^5 cm^{-1}), and a-Si:H (offset by 10^5 cm^{-1}).

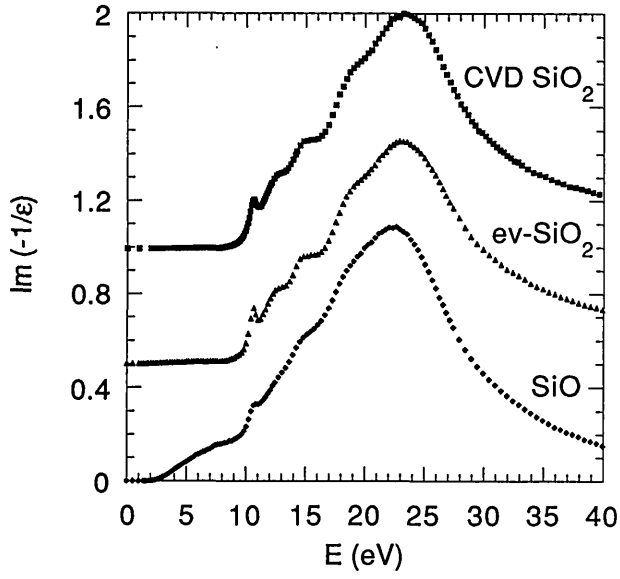

Fig. 5. Absolute energy loss functions for a-SiO, evaporated SiO_2 (offset by 0.5), and CVD-SiO_2 (offset by 1.0).

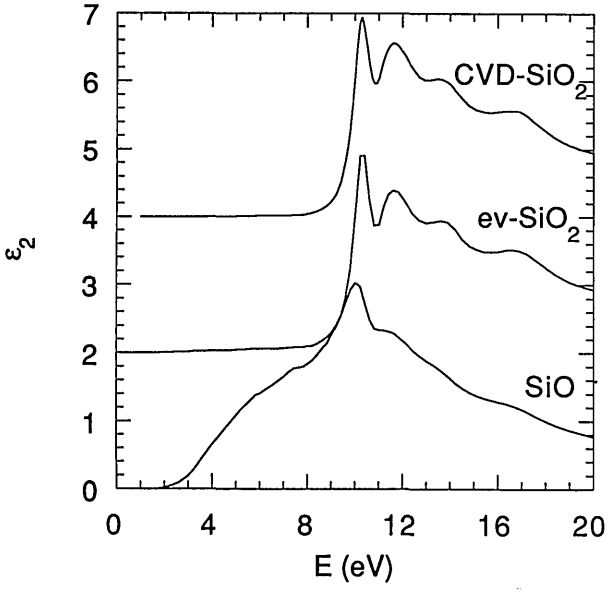

Fig. 6. ϵ_2 spectra of a-SiO, evaporated SiO_2 (offset by 0.5), and CVD SiO_2 (offset by 1.0).

11.5, 13.6, and 16.5 eV. Features are also apparent at 6.0 and 7.5 eV, below the SiO_2 absorption threshold.

The similarities in the spectra may indicate similarity in the electronic structure of the occupied or the unoccupied bands or both. Figure 7 shows the absorption coefficients of SiO and SiO_2 in the Si 2*p* core region. (The CVD and evaporated SiO_2 samples were virtually identical in this region, so only the CVD data are shown.) The core spectra, which probe the unoccupied electronic states, are quite similar. SiO shows broad absorption beginning at about 100 eV, approximately 0.5 eV above the Si threshold. The 2*p* absorption in SiO_2 begins at 105 eV. Both SiO and SiO_2 show a strong doublet at 105.8 and 106.4 eV, an excitonic transition split by the Si 2*p* spin-orbit splitting, and a single peak at 108.2 eV. The differences between these peaks and the peaks in the interband spectrum indicate a significant core exciton binding energy.

The similarity in the 2*p* core spectra may lead to the conclusion that the similarities in the valence spectra of SiO and SiO_2 are due to similar conduction band structures. This in turn would indicate that the valence absorption arises from a single occupied state. However, the work of Nithianandam and Schnatterly[18] indicates that the valence absorption is due to transitions from different valence bands into the same conduction band. From this we may conclude that SiO and SiO_2 have similar band structures in both the valence and conduction bands.

The extent of the similarities between the band structures of the two different silicon oxides may come as somewhat of a surprise. However, several studies have come to the conclusions that variation of the concentration of O in SiO_x compounds does not shift peaks in the density of states but changes only the amplitudes of the peaks.[34-36] This is a result of both the constituent ions and the structure. The structure of the various polymorphs of SiO_2 is based on SiO_4 tetrahedra. When the amount of O is varied, this can be modeled by $Si–Si_yO_{4-y}$ tetrahedra, which causes only a small perturbation in the structure. Since the family of compounds fits well into the tight-binding scheme, the atomic orbitals composing the solid-state bands also do not change, leading to little change in the shapes of the energy levels arising from the Si–O bonds. The added strength below the SiO_2 absorption threshold in both the valence and core regions comes from orbitals mostly comprising Si–Si bonds.

Our SiO_2 spectra show significant losses beginning at ~1.5 eV in the evaporated sample and 2.8 eV in the CVD sample. This obviously arises from the preparation of thin-film samples. The electron-beam evaporation quite likely results in O-deficient samples, while the CVD process may lead to nonstoichiometric samples or significant H content. Our loss spectra show peaks at 6.5 eV in both CVD and evaporated materials. This is the absorption energy of the *E'* center, a charged oxygen vacancy.[37] In the evaporated sample there is other structure below the band gap, which is similar to the shape of the SiO spectrum, indicating that there may be sufficient defect density to create small pockets of SiO. Above 9 eV our

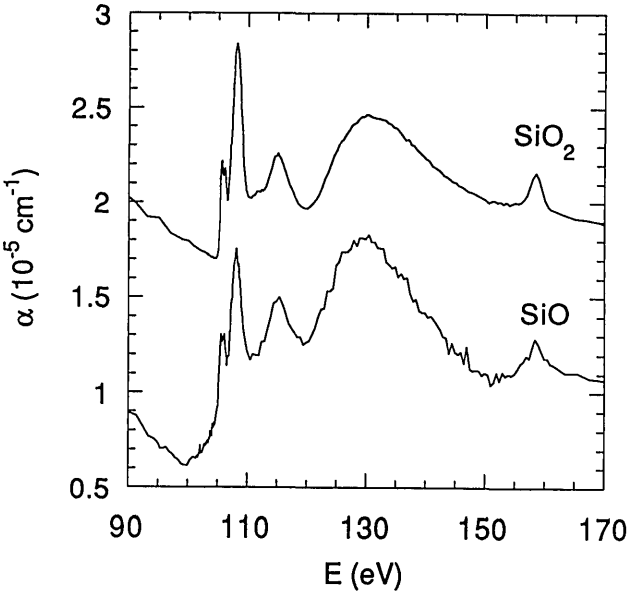

Fig. 7. Absorption coefficient of SiO and CVD-SiO_2 (offset by 10^5 cm^{-1}).

spectra are in good agreement with a recent band structure calculation of α-quartz.[38] All the peaks in the calculation are present in our spectra as either peaks or shoulders, and we have an additional shoulder at 12.5 eV not present in the α-quartz calculation.

CONCLUSIONS

We have reported the first measurements of the optical properties of Si and its oxides covering the range from IR to soft x ray on a single instrument. Our results are in agreement with previous results, where available. Amorphous Si lacks the fine structure of the crystalline Si spectrum in both the interband region and the $2p$ region. The properties of SiO and SiO_2 are remarkably similar above the SiO_2 band gap.

ACKNOWLEDGMENTS

This research is supported in part by National Science Foundation grant DMR 88-19052. We thank other members of our group, R. Carson, D. Husk, S. Velasquez, and E. Benitez, for helpful discussions.

*Present address, Electron and Optical Physics Division, National Institute of Standards and Technology, Gaithersburg, Maryland 20899.

REFERENCES

1. H. Bichsel, "Straggling in silicon detectors," Rev. Mod. Phys. **60,** 633–700 (1988).
2. E. L. Benitez, D. E. Hust, C. Tarrio, and S. E. Schnatterly, "Surface recombination effects in soft x-ray efficiencies," Appl. Phys. Lett. **59,** 396–398 (1991).
3. H. R. Philipp and E. A. Taft, "Optical constants of silicon in the region 1 to 10 eV," Phys. Rev. **120,** 37–38 (1960).
4. G. Weiser, D. Ewald, and M. Milleville, "Reflectivity and dielectric function of glow-discharge silicon," J. Non-Cryst. Solids **35–36,** 447–452 (1980).
5. G. D. Cody, B. Abeles, C. R. Wronski, B. Brooks, and W. A. Lanford, "Optical absorption of $SiH_{0.16}$ films near the optical gap," J. Non-Cryst. Solids **35–36,** 463–468 (1980).
6. D. E. Aspnes and A. A. Studna, "Dielectric functions and optical parameters of Si, Ge, GaP, GaAs, GaSb, InP, InAs, and InSb from 1.5 to 6.0 eV," Phys. Rev. B **27,** 985–1009 (1983).
7. D. Aspnes, A. A. Studna, and E. Kinsbron, "Dielectric properties of heavily doped crystalline and amorphous silicon from 1.5 to 6.0 eV," Phys. Rev. B **29,** 768–779 (1984).
8. B. Drevillon, "*In situ* studies of the growth of hydrogenated amorphous silicon," J. Non-Cryst. Solids **114,** 139–144 (1989).
9. J. Stiebling, "Optical properties of monocrystalline silicon by electron energy loss measurements," J. Phys. B **31,** 355–357 (1978).
10. J. Stiebling and H. Raether, "Dispersion of the volume plasmon of silicon at large wave vectors," Phys. Rev. Lett. **40,** 1293–1295 (1978).
11. C. H. Chen, A. E. Meixner, and B. M. Kincaid, "Bulk plasmon dispersion in silicon $0 < q < 1.5\ k_F$," Phys. Rev. Lett. **44,** 951–954 (1980).
12. F. C. Brown and O. P. Rustgi, "Extreme ultraviolet transmission of crystalline and amorphous silicon," Phys. Rev. Lett. **28,** 497–500 (1972).
13. F. C. Brown, R. Z. Bachrach, and M. Skibowski, "L_{23} threshold spectra of doped silicon and silicon compounds," Phys. Rev. B **15,** 4781–4788 (1977).
14. P. E. Batson, K. L. Kavanaugh, C. Y. Wong, and J. M. Woodall, "Local bonding and electronic structure obtained through electron energy loss scattering," Ultramicroscopy **22,** 89–101 (1987).
15. H. R. Philipp, "Optical properties of noncrystalline Si, SiO, SiO_x, and SiO_2," J. Phys. Chem. Solids **32,** 1935–1945 (1971).16.U. Buechner, "The dielectric function of mica and quartz determined by electron energy losses," J. Phys. C **8,** 2781–2787 (1975).
17. W. M. Skiff and R. W. Carpenter, "Near-edge fine structure analysis of core-shell electronic absorption edges of Si and its refractory compounds using electron energy loss microscopy," J. Appl. Phys. **62,** 2439–2449 (1980).
18. V. J. Nithianandam and S. E. Schnatterly, "Soft x-ray emission and inelastic electron scattering study of the electronic transitions in amorphous and crystalline SiO_2," Phys. Rev. B **38,** 5547–5553 (1988).
19. Z. A. Weinberg, G. W. Rubloff, and E. Bassous, "Transmission, photoconductivity, and the experimental band gap of thermally grown SiO_2 films," Phys. Rev. B **19,** 3107–3117 (1979).
20. I. T. Godmanis, A. N. Trukhin, and K. Hubner, "Exciton-phonon interaction in crystalline and vitreous SiO_2," Phys. Status Solidi B **116,** 279–287 (1983).
21. S. K. J. Al-Ani, C. A. Hogarth, and D. N. Waters, "Effect of temperature on the optical absorption edge of amorphous films of SiO," Phys. Status Solidi B **123,** 653–658 (1984).
22. S. E. Schnatterly, "Inelastic electron scattering spectroscopy," in *Solid State Physics*, H. Ehrenreich, F. Seitz, and D. Turnbull, eds. (Academic, New York, 1979), Vol. 34.
23. D. Y. Smith, "Dispersion theory, sum rules, and their application to the analysis of optical data," in *The Handbook of Optical Constants*, E. R. Palik, ed. (Wiley, New York, 1986), Chap. 3.
24. P. C. Gibbons, J. J. Ritsko, and S. E. Schnatterly, "Inelastic electron scattering spectrometer," Rev. Sci. Instrum. **46,** 1546–1554 (1975).
25. P. Livins, T. Aton, and S. E. Schnatterly, "Inelastic electron scattering in amorphous Si_3N_4 and Al_2O_3 with multiple-scattering corrections," Phys. Rev. B **37,** 5511–5519 (1988).
26. J. D. Cohen, D. V. Lang, and J. P. Harbison, "Direct measurement of the bulk density of gap states in n-type hydrogenated amorphous silicon," Phys. Rev. Lett. **45,** 197–200 (1980).
27. H. Raether, *Excitation of Plasmons and Interband Transitions by Electrons*, Vol. 88 of Springer Tracts in Modern Physics (Springer-Verlag, Berlin, 1979), p. 9.
28. J. Hubbard, "The description of collective motions in terms of many-body perturbation theory. II: The correlation energy of a free-electron gas," Proc. R. Soc. London Ser. A **243,** 336–352 (1957).
29. P. Nozieres and D. Pines, "Correlation energy of a free-electron gas," Phys. Rev. **111,** 442–454 (1958).
30. P. Livins and S. E. Schnatterly, "Shake-up in soft x-ray emission II: plasmon satellites in XPS," Phys. Rev. B **37,** 642–649 (1988).
31. H. Piller, in Ref. 23, pp. 571–586.
32. H. Ma, S. H. Lin, R. W. Carpenter, and O. F. Shakey, "Theoretical comparison of electron energy loss and x-ray absorption near-edge structure of the Si L_{23} edge," J. Appl. Phys. **68,** 288–290 (1990).
33. M. Altarelli and D. L. Dexter, "Core excitons and the soft x-ray threshold of silicon," Phys. Rev. Lett. **29,** 1100–1103 (1972).
34. E. Martinez and F. Yndurain, "Realistic model for the electronic structure of amorphous SiO_x alloy," Solid State Commun. **37,** 979–982 (1982); "Theoretical study of the electronic structure of SiO_x," Phys. Rev. B **24,** 5718–5725 (1981).
35. R. Strehlow and W. H. Lamfried, "A new approach to the electronic structure of SiO_x," Phys. Status Solidi B **109,** 75–79 (1982); "On the electronic structure of SiO_x-random bonding model," Phys. Status Solidi B **114,** 165–170 (1982).
36. W. Y. Ching, "Theory of amorphous SiO_2 and SiO_x I," Phys. Rev. B **26,** 6610–6621 (1982); "Theory of amorphous SiO_2 and SiO_x II," Phys. Rev. B **26,** 6622–6632 (1982); "Theory of amorphous SiO_2 and SiO_x III," Phys. Rev. B **26,** 6633–6641 (1982).
37. F. J. Feigl, W. B. Fowler, and K. L. Yip, "Oxygen-vacancy model for the E_1' center in SiO_2," Solid State Commun. **14,** 225–229 (1974).
38. Y. Xu and W. Y. Ching, "Electronic and optical properties of all polymorphic forms of SiO_2," Phys. Rev. B **44,** 11048–11059 (1991).